Biomacromolecules

pubs.acs.org/Biomac

Article

Optical Control of Cytokine Signaling via Bioinspired, Polymer-Induced Latency

Lacey A. Perdue, Priscilla Do, Camille David, Andrew Chyong, Anna V. Kellner, Amanda Ruggieri, Hye Ryong Kim, Khalid Salaita, Gregory B. Lesinski, Christopher C. Porter, and Erik C. Dreaden*

Cite This: *Biomacromolecules* 2020, 21, 2635−2644

Read Online

ACCESS | Metrics & More | Article Recommendations | Supporting Information

ABSTRACT: Cytokine signaling is challenging to study and therapeutically exploit as the effects of these proteins are often pleiotropic. A subset of cytokines can, however, achieve signal specificity via association with latency-inducing proteins, which cage the cytokine until disrupted by discreet biological stimuli. Inspired by this precision, here, we describe a strategy for synthetic induction of cytokine latency via modification with photolabile polymers that mimic latency while attached then restore protein activity in response to light, thus controlling the magnitude, duration, and location of cytokine signals. We characterize the high dynamic range of cytokine activity modulation and find that polymer-induced latency, alone, can prolong in vivo circulation and bias receptor subunit binding. We further show that protein derepression can be achieved with a near single-cell resolution and demonstrate the feasibility of transcutaneous photoactivation. Future extensions of this approach could enable multicolor, optical reprogramming of cytokine signaling networks and more precise immunotherapies.

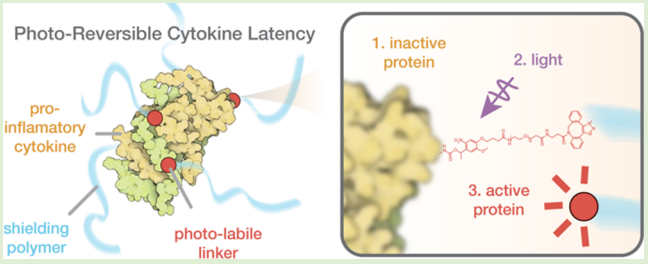

Downloaded via EMORY UNIV on August 5, 2020 at 13:55:07 (UTC).
See https://pubs.acs.org/sharingguidelines for options on how to legitimately share published articles.

INTRODUCTION

Cytokine signaling is critically important to a variety of physiological processes, including cell and tissue development, aging, disease pathogenesis, and the mounting of effective innate or adaptive immune responses.[1−3] In addition to serving as signal mediators, these proteins can also act as potent therapies with more than 18 cytokine products currently FDA-approved for the treatment of diseases, including chronic hepatitis, multiple sclerosis, rheumatoid arthritis, chronic kidney disease, degenerative disk disease, and multiple types of cancer. Although cytokines hold great potential as tools to both study and treat human disease, in vivo effects of these proteins are often highly pleiotropic and thus difficult to understand and challenging to control.[4]

One mechanism by which cytokines with diverse effects can transmit tissue- and cell-specific information is via expression in an inactive, or *latent,* form in which the protein is sterically shielded by another peptide or protein binding partner. Transforming growth factor-β1 (TGF-β1), for example, has recently been shown to noncovalently associate with a latency-associated peptide (LAP), which deshields from TGF-β1 in response to traction forces caused by the binding of αVβ6 or αVβ8 integrins with either cell membrane-bound GARP (glycoprotein A repetitions predominant) or extracellular matrix-bound LTBP-1 (latent transforming growth factor beta-binding protein 1).[5] This stimuli-responsive uncaging of the protein can lead to remarkable specificity; interaction with migratory dendritic cells has been shown to present TGF-β1 to naïve CD8$^+$ T cells, preconditioning them for tissue-resident memory fate.[6] Similarly, the interaction with regulatory T cells (Tregs)[7] and microglia[8] has been found to deshield TGF-β1, thus initiating anti-inflammatory signaling cascades in these cells and other nearby cell types.

Inspired by the ability of reversible shielding to impart cell- and tissue-specificity to cytokines expressed in a latent form, we hypothesized that chemical modification with synthetic macromolecules could impart similar or improved specificity to other cytokines not expressed in a latent state. Photoresponsive linker technologies present a potential, synthetic alternative to latency binding proteins, providing spatiotemporal control over cytokine activation and, additionally, orthogonality to existing shielding/deshielding pairs. Historically, photolabile linkers have been utilized to reversibly immobilize peptides and oligonucleotides onto purification resins; however, more recently, this approach has been adapted in order to reversibly cage small molecules, peptides, and nucleic acids.[9,10] For example, caged neurotransmitters have been used to study memory formation in the brain,[11] caged peptides complexed with a major histocompatibility complex (MHC) have been

Received: February 24, 2020
Revised: May 5, 2020
Published: May 6, 2020

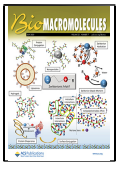

© 2020 American Chemical Society

https://dx.doi.org/10.1021/acs.biomac.0c00264
Biomacromolecules 2020, 21, 2635−2644

exploited to study structural reorganization at the immune synapse,[12] and caged single guide RNA (sgRNA) has been utilized to spatially constrain gene editing by CRISPR/Cas9.[13] Extension of this strategy to immune signaling proteins—which can be hundreds of times larger—thus represents a significant and unaddressed challenge.

Here, we describe a strategy whereby cytokines are chemically modified with photolabile polymers that mimic the induction of protein latency while attached then deshield to recover the protein activity in response to monochromatic light exposure. This approach enables both the magnitude and the duration of cytokine signals to be tuned on demand, with high spatial resolution, and can be rapidly adapted to a range of additional cytokine or chemokine proteins. Future extensions of this approach could enable optical reprogramming of cytokine signaling networks and could lead to new immunotherapies that are more tissue-specific and patient-personalized.

METHODS

Materials and Supplies. Unless otherwise specified, reagents were used as received without further purification. Recombinant human IL-2 (200-02, Peprotech), recombinant human IL-15 (570,308, Biolegend), and recombinant mouse scIL-12 (130-096, Miltenyi Biotech) were sourced as indicated. Sulfo-Cyanine7 NHS ester (Lumiprobe), DBCO-NHS ester (1160, Click Chemistry Tools), poly(ethylene glycol) methyl ether azide (20 kDa, Nanocs), polyacrylamide gels (Bio-Rad, 4−15 wt%), and IFNγ ELISA (DY485, R&D Systems) were sourced as indicated.

Photoinduced Polymer Cleavage. Detailed characterization of light-induced polymer cleavage was monitored via fluorescence dequenching of 5FAM- and CPQ2-modified polyethylene glycol (5 kDa). Polymers containing the photolabile linkers shown in Figure S1b were obtained from CPC, Inc. using linker reagents obtained from Advanced Chemtech. Modified polymers (azido-G-K(CPQ2)-NB/DMNB-PEO4-G-K(5FAM)-G-C-PEG5k) were >96% pure as measured by RP-HPLC. Samples were dissolved in 500 nM ultrapure water and irradiated within quartz cuvettes using collimated, light-emitting diodes (Solis, Thorlabs). Fluorescence dequenching was measured on a Spectramax Id3 plate reader (Molecular Devices). Cleavage kinetics were fit to a one-phase decay using Graphpad Prism software. Storage and stability measurements were similarly obtained from solution aliquots maintained in on a laboratory benchtop, heated incubator, or laboratory refrigerator. Samples were covered with aluminum plate films or tissue phantoms and exposed to fluorescent, overhead office lights as indicated.

Polymer-Induced Latency. Recombinant cytokines were sequentially modified with photolabile linkers and polymers via carbodiimide coupling and Cu-free click chemistry, respectively. Briefly, cytokines were reacted with a commercial 2-nitrobenzyl linker displaying both NHS ester and DBCO substituents (1160-10, Click Chemistry Tools) followed by addition of poly(ethylene glycol) methyl ether azide. Proteins were purified via a desalting column (7 k MWCO, Pierce) or, during optimization, with DBCO agarose beads (Click Chemistry Tools), following the manufacturer's instructions. DBCO agarose beads (3 equiv relative to azide) were incubated with protein conjugates overnight at 4 °C with rotary agitation (800 rpm). Unless stated otherwise, reaction conditions are described as molar equivalents relative to total lysine residues or total DBCO groups.

Recombinant IL-2 was modified via dilution in a 150 mM sodium phosphate buffer (pH 8.5) containing 0.5 mM SDS and addition of 3 equiv of photolabile linker to a maximum DMSO concentration of 5% v/v. Then, 10 equiv of poly(ethylene glycol) methyl ether azide (20 kDa) dissolved in PBS (pH 7.4) was added and allowed to react. All cytokine modification steps were allowed to proceed overnight at 4 °C with rotary agitation (800 rpm).

Recombinant scIL-12 was modified via dilution in a 150 mM sodium phosphate buffer (pH 8.5) containing 0.5 mM SDS and addition of (i) 1 equiv of NHS-SulfoCy7 to 5% v/v DMSO or (ii) addition of 1 equiv of NHS-SulfoCy7 and 5 equiv of a photolabile linker to 5% v/v DMSO. Then, 5 equiv of poly(ethylene glycol) methyl ether azide (20 kDa) dissolved in PBS (pH 7.4) was added and allowed to react.

Recombinant IL-15 was modified via dilution in a buffer containing 10 mM NaH_2PO_4/150 mM NaCl and addition of 20 equiv of a photolabile linker to 5% v/v DMSO.

Protein Characterization. Cytokine hydrodynamic size was measured by dynamic light scattering (Wyatt DynaPro Plate Reader III) using 2−4 averages of 10−30 s acquisitions. Electrophoretic mobility was measured via polyacrylamide gel electrophoresis under reducing conditions (50 mM dithiothreitol, Bio-Rad). Protein bands were visualized with a Coomassie G250 stain (Bio-Rad) and imaged using a Licor CLx gel imager.

Cytokine-Induced Proliferation. Murine CTLL-2 T cells (ATCC) were maintained in RPMI 1640 with high glucose, L-glutamine, and HEPES and supplemented with 10% heat inactivated FBS, 10% rat T-STIM (Corning), 2 mM L-glutamine, and 1 mM sodium pyruvate. To examine the cytokine activity, cells were washed in assay media (maintenance media without T-STIM) and plated in assay media at $1.5x10^3$ cells per well within a 96-well plate. Wells were then treated for 24 h with equimolar amounts of wild-type or latent protein that was LED-exposed for the indicated time/irradiance. Cell proliferation was measured using a CellTiter-Glo 2.0 reagent (Promega) following the protocol provided by the manufacturer. Cell lines were routinely screened for mycoplasma (MycoAlert Plus, Lonza).

Antigen-Specific T Cell Activation. OT-I mouse (6−8 weeks) splenocytes were isolated using Ficoll−Paque following mechanical homogenization and PBS washing of excised spleen tissues. Splenocytes were resuspended in RPMI 1640 (ATCC) containing 10% FBS and 100 U/mL of penicillin G and streptomycin. For stimulation, cells were incubated with 10 nM chicken egg ovalbumin peptide 257−264 (SIINFEKL, Invivogen) with or without 1000 IU/mL of IL-2 (or equimolar amounts modified protein) and plated at $2x10^6$ cells/well within a 96-well plate. After 24 h, the cell culture supernatant was harvested and tested for IFNγ secretion via ELISA (R&D Systems). Optical density at 450 nm was measured using a Spectramax Id3 plate reader (Molecular Devices), and results were compared with standard curves. These studies were approved by Emory University's Institutional Animal Care and Use Committee.

JAK/STAT Pathway Activation. STAT5:SEAP reporter cells (HKB-il2, Invivogen) were maintained in DMEM supplemented with 4.5 g/L of glucose, 2−4 mM L-glutamine, 10%v/v heat-inactivated FBS, 100 U/mL of penicillin, 100 μg/mL of streptomycin, 100 μg/mL of Normocin, and HEK blue selection media (Invivogen). For assays, $5x10^4$ cells were plated in complete growth media, without selection antibiotics, within 96-well plates and treated with equimolar amounts of wt or latent IL-2 (1000 IU/mL or equimolar amounts modified protein) for 48 h. Then, 20 μL of cell culture supernatant was withdrawn and analyzed for the alkaline phosphatase content via change in QUANTI-Blue (Invivogen, rep-qbs) absorbance at 620 nm (Spectramax id3 plate reader).

Binding Affinity. Cytokine and cognate receptor binding kinetics were measured via biolayer interferometry using an Octet RED384 system (ForteBio). Nickel nitrilotriacetic acid sensors (Ni−NTA, ForteBio) were equilibrated in PBS and coated with polyhistidine-tagged receptor proteins (SinoBiological) for 5 min (1.5 μg/mL IL-2Rα, 3.3 μg/mL IL-2Rβ). Association kinetics were measured over 5 min at 2.0 μM IL-2 followed by dissociation in PBS over 5 min. Measurements were repeated in three independent experiments and fit using Data Analysis 8.0 (ForteBio) using a 1:1 kinetic model.

Pharmacokinetics. C57BL/6 mice (female, 7 weeks) were injected via the tail vein with 2 μg scIL-12 protein conjugated with Cy7 alone or Cy7 with photolabile poly(ethylene glycol). Plasma was collected from 100 μL of blood obtained via submandibular bleed into heparinized tubes (BD Microtainer). Plasma fluorescence was integrated using ImageJ software after polyacrylamide gel electrophoresis. Mice with peak plasma fluorescence <1.2× above the baseline were excluded. These studies were approved by Emory University's Institutional Animal Care and Use Committee.

https://dx.doi.org/10.1021/acs.biomac.0c00264
Biomacromolecules 2020, 21, 2635−2644

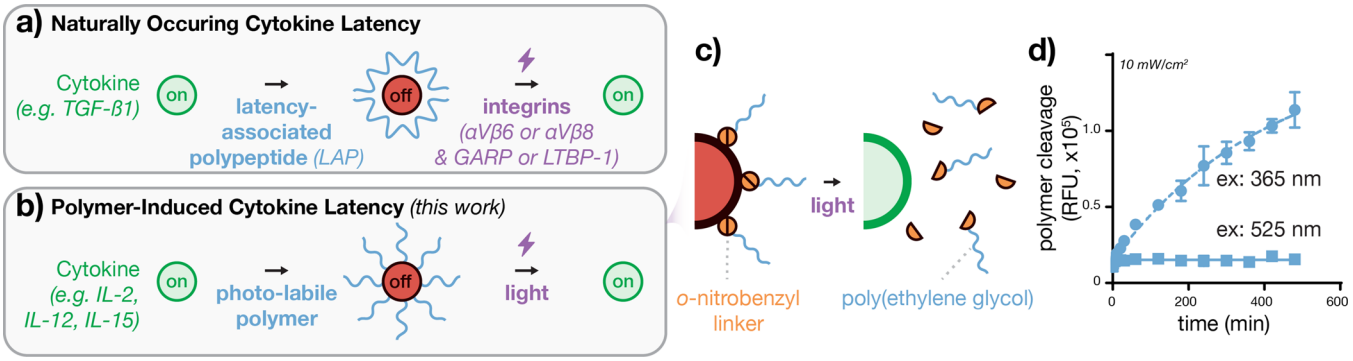

Figure 1. Bioinspired cytokine latency via photolabile polymer modification. (a) Transforming growth factor-β1 (TGF-β1) transmits tissue- and cell-specific cytokine signals via association with a latency-associated peptide (LAP), which sterically shields and later disassociates from TGF-β1 in response to traction forces caused by the binding of αVβ6 or αVβ8 integrins with either cell membrane-bound GARP or extracellular matrix-bound LTBP-1. (b) Strategy for the induction of reversible latency in cytokines with pleiotropic effects via modificaiton with end-modified, photolabile polymers. (c) Illustration of the traceless modification strategy used here whereby 20 kDa poly(ethylene glycol) polymer chains are appended to cytokine lysine residues via *o*-nitrobenzyl groups, which are (d) rapidly degraded by blue, but not green, LED light as measured by cleavage-induced fluorescence dequenching. Data in panel (c) represent mean ± SD of three technical replicates.

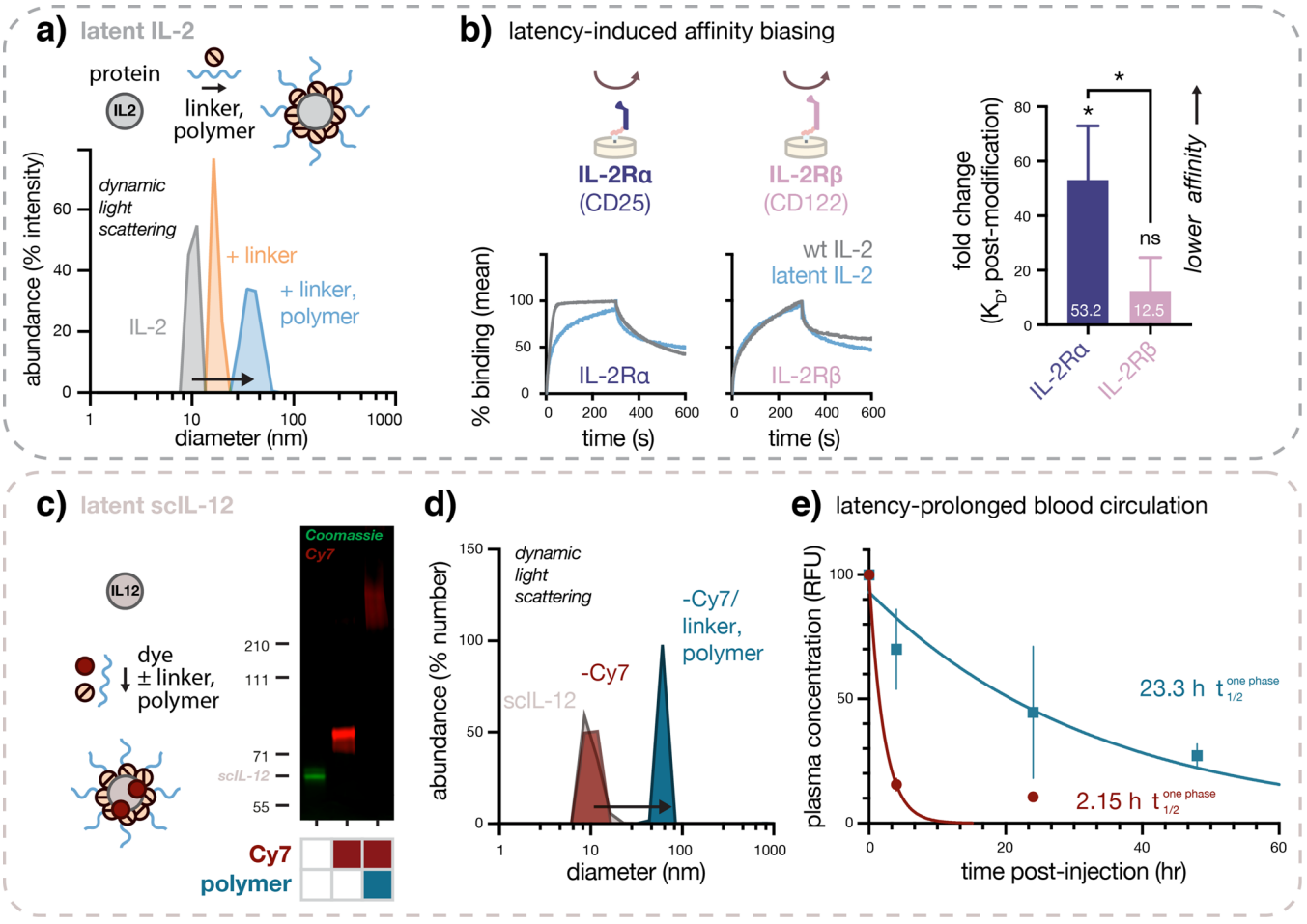

Figure 2. Polymer-induced latency augments cytokine size, biases receptor subunit binding affinity, and prolongs in vivo circulation. (a) Stepwise increase in IL-2 hydrodynamic size upon linker and polymer conjugation as measured by dynamic light scattering [diameter in nm, (Polydispersity index): 11.5 (0.1), 17.1 (0.1), 38.5 (0.2)]. (b) Sensorgrams depicting binding kinetics for IL-2 or latent IL-2 association/dissociation with IL-2Rα (CD25) or IL-2Rβ (CD122). (Inset) Fold change in postmodification binding affinity. (c) Electrophoretic mobility shift demonstrating Cy7 dye- and polymer- dependent modification of scIL-12 as measured by polyacrylamide gel electrophoresis. (d) Increase in scIL-12 hydrodynamic size following Cy7 conjugation with or without linker/polymer modification as measured by dynamic light scattering. (e) Plasma pharmacokinetics of Cy7-labeled scIL-12 modified with or without a linker/polymer following intravenous injection into C57BL/6 mice, illustrating prolonged circulation following photolabile polymer modification. Data in panel (b) represent mean ± SD of three technical replicates. Data in panel (e) represent mean ± SEM of two to three biological replicates. Curve fits in panel (e) were constrained to decay to average fluorescence values from vehicle-treated mice. Error bars in panel (e) smaller than data point sizes are obscured. $p < .05$(*), $p < .01$(**), $p < .001$(***), $p < .0001$(****).

https://dx.doi.org/10.1021/acs.biomac.0c00264
Biomacromolecules 2020, 21, 2635−2644

Tissue Phantoms. Polydimethylsiloxane (PDMS) tissue phantoms were prepared as described previously.[14−16] Briefly, a Sylgard 184 elastomer and curing agent (Dow Corning) were doped with titanium dioxide (0.3−1.0 μm rutile, Atlantic Equipment Engineers) and India ink (Higgins 44201) to concentrations that approximate attenuated light transmission through human tissue (1.68% transmission of 365 nm light through epidermis, dermis, and 2 mm through hypodermis tissue, respectively).[17] Solutions were degassed and sequentially cast into rectangular silicone molds prior to measurement of LED light transmission using a thermal power sensor (ThorLabs). Mean light transmission through epidermis, dermis, and adipose tissue (2 mm) was measured as 3.04%. Photoinduced heating measurements were collected using a FLIR ONE Pro thermal imaging camera and analyzed using Vernier Thermal Analysis Plus software. Inferences regarding heat pain responses assume a normal skin surface temperature of 33−34 °C and a heat pain threshold of 42−45 °C.

Statistical Analysis. All p values were calculated using either two-way ANOVA with Tukey post hoc correction or a two-way t test, depending on the sample number, using Graphpad Prism software unless otherwise specified.

Photo-Patterned Protein Activation. Silicone cell isolators (Electron Microscopy Sciences) were adhered to aldehyde-functionalized glass slides (Nanocs) and coated overnight in 2 mg/mL of BSA (VWR) at room temperature (RT). Coated wells were then washed 2× with 0.2% SDS and 2× with deionized water. The protein was covalently bound to the slide surface via addition of freshly prepared 2.5 mg/mL of $NaBH_4$ (Sigma) dissolved in 25%v/v ethanol in PBS at RT for 5 min. Wells were again washed 3× with 0.2% SDS and 3× with deionized water. DBCO−sulfo−NHS ester (Sigma) in PBS was added at 5 equiv (relative to lysine residues) for 4 h at RT, then wells were again washed 3× with deionized water. Azide-PC-Biotin (Click Chemistry Tools) dissolved in DMSO was added to the wells at 1 equiv (relative to DBCO groups) and incubated overnight at RT. Wells were washed 3× with deionized water and filled with 50% glycerol prior to UV exposure through custom, chrome-patterned quartz photomasks (Front Range Photomask) for 30 min with a 365 nm LED (Thor Labs) at 30 mW/cm^2. Wells were washed 6× with deionized water, 3× with 0.2% SDS, and again 3× with deionized water. Streptavidin-FITC (Southern Biotech) in PBST (0.1% Tween 20) was incubated in the wells for 30 min at RT, then wells were washed 3× with PBST and 3× with deionized water. Cell isolators were removed, ProLong Diamond Antifade mounting media was added (Life technologies), and the slide was covered with a coverslip. The slide was visualized using a wide-field microscope with GFP filter settings (469/525 nm, Biotek Lionheart FX), and images were processed with Gen5 and ImageJ software.

RESULTS

Artificial Cytokine Latency Via Photolabile Polymer Modification. To assess the feasibility of polymer-induced cytokine latency and subsequent light-induced activation (Figure 1a−c), we first examined the cleavage efficiency of two distinct polyethylene glycol (PEG) polymers modified to exhibit fluorescence dequenching following the cleavage of o-nitrobenzyl linker derivatives when exposed with blue LED light (Figure S1a,b). In a phosphate buffer, these polymer cages exhibited fast cleavage kinetics ($k' \approx 0.028-0.12$ min^{-1}) that was both power-dependent and highly wavelength-discriminant (Figure 1d and Figure S1c−e). Based on these results, we devised a traceless[18−20] chemical modification strategy, which appended high molecular weight PEG (20 kDa) to cytokine lysine residues by way of a dialkoxy-substituted 2-nitrobenzyl linker (Figure S2) selected due to its redshifted absorption (Figure S3) and enhanced water solubility compared with other o-nitrobenzyl cages. These photolabile linkers are known to undergo a Norrish type II reaction upon light activation to liberate a CO_2 molecule and regenerate an amino group from corresponding carbamate adducts.

To demonstrate polymer-induced cytokine latency, we selected recombinant human IL-2 as a candidate for photolabile polymer modification due to its lack of a known latency binding partner and its well-described pleiotropic effects in vivo, for example, its simultaneous immunostimulatory effects exerted via cytotoxic T cells and immunosuppressive effects exerted through regulatory T cells. We also selected IL-2 as the protein that has demonstrated clinical benefits in patients with melanoma, renal cell cancer, and neuroblastoma. These benefits are greatly limited by the small size and rapid excretion of IL-2, which necessitates continuous or frequent high-dosing and thus toxicity and complex treatment management.[21,22] We hypothesized that polymer-induced IL-2 latency could be used to both control IL-2 signaling ex vivo and improve the safety or therapeutic potential of this and related cytokines via prolonged circulation.

Following modification of IL-2, we observed a stepwise increase in size upon both linker and polymer conjugation as measured by both polyacrylamide gel electrophoresis and dynamic light scattering (Figure 2a). Latent IL-2 was approximately threefold larger than the wild-type protein in overall diameter, thus well above the lower size limit for renal clearance in humans. We further examined the binding affinity of latent IL-2 with two of its cognate receptor subunits, IL-2Ra (CD25, rhIL-2−10^{-8} M) and IL-2Rb (CD122, rhIL-2−10^{-7} M) via biolayer interferometry (Figure 2b).[23] Strikingly, binding affinity of IL-2 toward IL-2Rα was decreased approximately 53-fold following latency induction (20 ± 7 μM), whereas affinity toward IL-2Rβ was nominally lower but failed to reach statistical significance (46 ± 40 μM). This serendipitous result suggests that, relative to wild-type IL-2, latent IL-2 maintains a biased activity toward CD8$^+$ T cells that express IL-2R$\beta\gamma$ and dampened activity towards immunosuppressive Tregs that constitutively express IL-2R$\alpha\beta\gamma$.[24]

Given that the off-target activity toward Tregs is believed to contribute, in part, to the failure of IL-2 therapy in patients,[25] these findings warrant future investigation in mouse models of cancer and other diseases reliant on T cell immune evasion.

Having demonstrated that polymer-induced latency can modulate cognate receptor binding affinity, we characterized the effect of polymer-induced latency on in vivo cytokine circulation using IL-12, another recombinant cytokine under clinical investigation, which similarly suffers from rapid clearance and systemic, off-target toxic effects.[26] As therapeutic cytokines are generally quite small (ca. 12−70 kDa), polymer modification—frequently, with PEG—is often used to decrease renal clearance, thus prolonging circulation and augmenting tissue exposure with drugs (e.g., pegfilgrastim, peginterferon, etc.).[27] To monitor cytokine circulation in vivo, we dye-labeled a novel single-chain variant of the cytokine, scIL-12, both with and without photolabile polymer modification (20 kDa PEG, Figure 2c). Cy7 labeling only nominally increased scIL-12 size as measured by polyacrylamide gel electrophoresis and dynamic light scattering, whereas combined dye and photolabile polymer modification increased the hydrodynamic size to 44 nm (Figure 2d), well above the renal clearance size threshold in humans and rodents. We then monitored the circulation of latent scIL-12 following tail vein injection in C57BL/6 mice, finding that the latent cytokine experienced an 11-fold increase in the circulation half-life following polymer-modification (Figure 2e). While we observed no large protein aggregates in DLS or electrophoretic mobility measurements of both latent cytokines, we do note that the formation of discreet protein multimers is commonly

https://dx.doi.org/10.1021/acs.biomac.0c00264
Biomacromolecules 2020, 21, 2635−2644

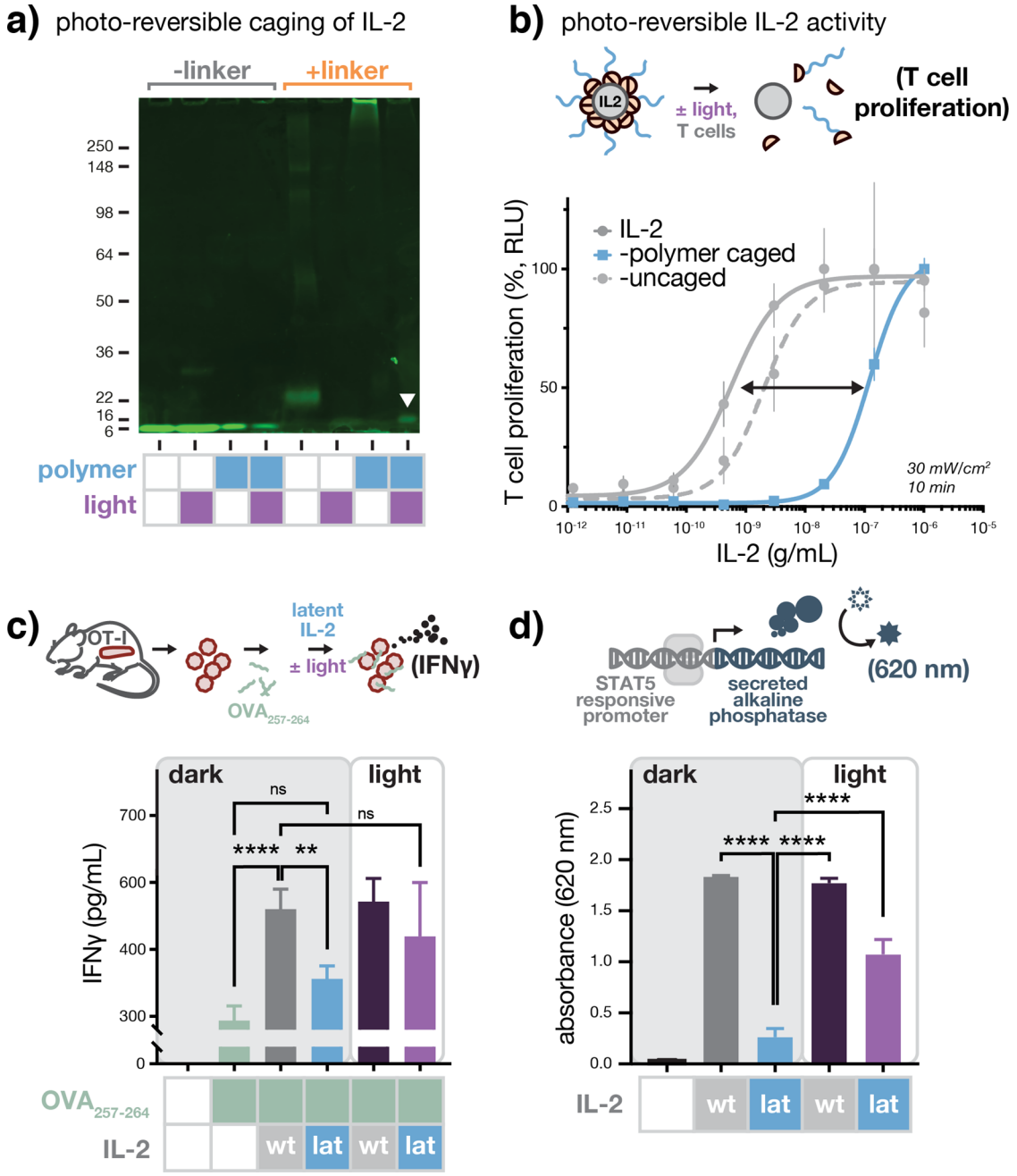

Figure 3. Photoexposure of latent IL-2 restores the protein size and functional activity. (a) Electrophoretic mobility shift demonstrating linker- and polymer-dependent modification of IL-2 and light-dependent restoration (arrowhead) of wild-type protein mobility as measured by polyacrylamide gel electrophoresis. (b) Polymer-dependent repression and light-induced restoration of IL-2 activity as measured by CTLL-2 T cell proliferation (24 h). Effect of latent IL-2 and uncaged IL-2 (1000 IU/mL molar equivalents) on (c) $OVA_{257-264}$ antigen-specific T cell activation and (d) JAK/STAT pathway activation as measured ex vivo by ELISA of OT-I splenocyte-secreted interferon gamma (IFNγ, 24 h) and STAT5 reporter cell secretion of aklakine phosphatase (48 h), respectively. Chromogenic substrate absorption in panel (d) was monitored at 620 nm. Data in panels (b) and (d) represent mean ± SD of three technical replicates, and data in panel (c) represent mean ± SD of of 6 technical replicates. $p < .01$(**), $p < .0001$(****).

observed among clinically approved cytokine therapies, both wild type and PEGylated,[28] and that we cannot exclude the possibility of dye- or polymer-induced multimer formation here, which might affect associated activity or abundance measurements. Physical state notwithstanding, these results suggest that the prolonged circulation of scIL-12 may (i) obviate the need for frequent, high dosing and (ii) improve tissue accumulation of the drug in therapeutic settings.

Photoactivation of Latent Cytokines. After characterizing the effects of polymer-induced cytokine latency, we next examined the recovery of functional protein activity using CTLL-2 T cells that depend on both IL-2 and IL-2Rα for growth.[29] Following latency-induction, we observed an approximate 10^3-fold drop in rhIL-2 activity as measured by CTLL-2 T cell proliferation (24 h); however, subsequent LED irradiation to uncage IL-2 near fully restored both native molecular weight and capacity for induced T cell proliferation (Figure 3a,b). Here, irradiation conditions were modeled after those used with common dental light curing units that operate over similar timescales (20−40 s) and with similar wavelengths

https://dx.doi.org/10.1021/acs.biomac.0c00264
Biomacromolecules 2020, 21, 2635−2644

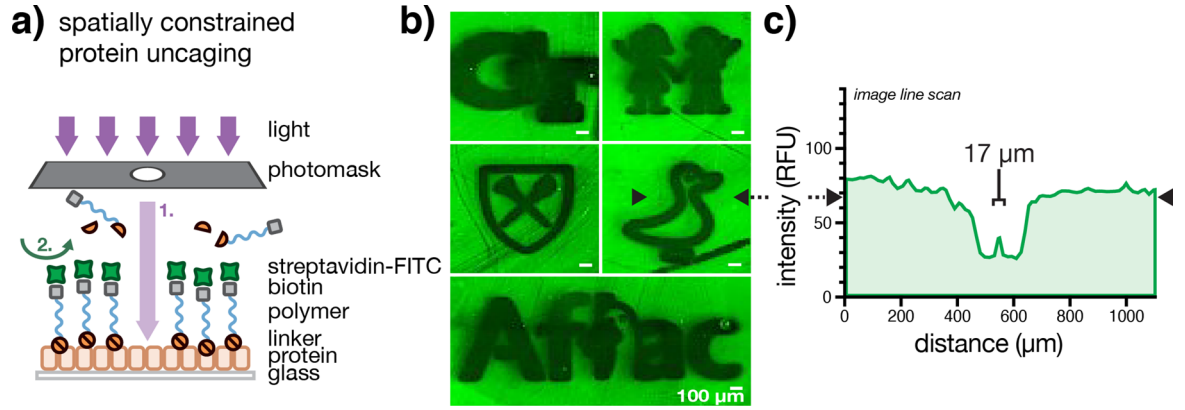

Figure 4. Light-induced uncaging enables precise, local control of protein activity. (a) Illustration of experiments to visualize protein latency and photoinduced derepression. (b) Fluorescence micrographs and (c) corresponding image line scan image indicating regions of latent (green) and uncaged (black) protein as measured by epifluorescence microscopy.

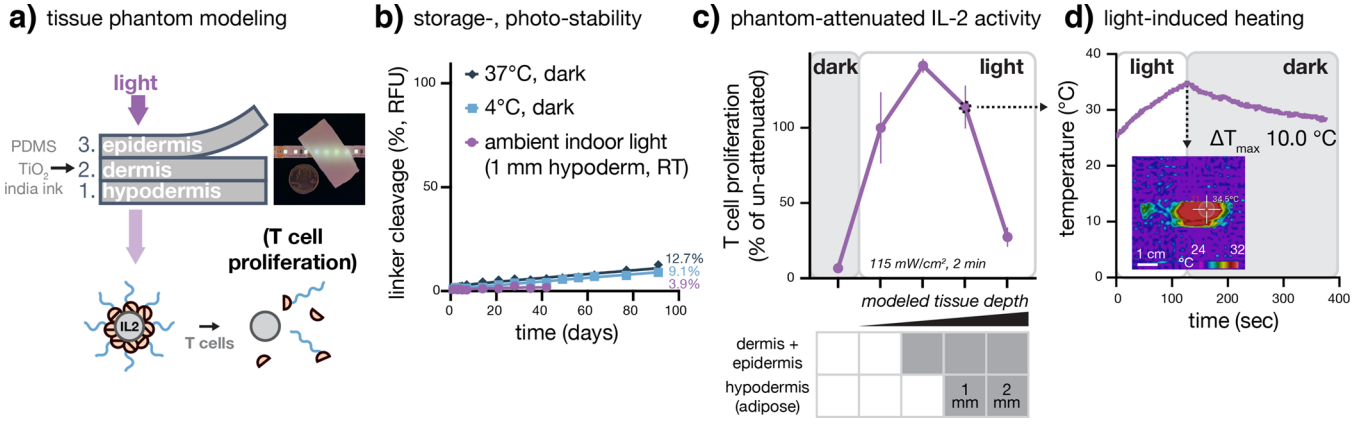

Figure 5. Latent IL-2 is stable and feasibly photoactivated through tissue models. (a) Illustration of multilayered tissue phantom construction. (b) Stability of 5 kDa poly(ethylene glycol) polymer photocages under prolonged, aqueous storage and under conditions simulating ambient, indoor light exposure of superficial veins (1 mm depth) as measured by cleavage-induced fluorescence dequenching. (c) Effect of tissue phantom light attention on latent IL-2 activity as measred by CTLL-2 T cell proliferation (24 h). (d) Superficial heating of multilayered tissue phantoms of the indicated thickness as measured by forward-looking infrared imaging. Data in panel (c) represent mean ± SD of three technical replicates. $p < .05$(*), $p < .01$(**), $p < .001$(***), $p < .0001$(****).

and power densities (400 nm, 300 mW/cm^2, respectively).[30] In vivo, as little as a 10-fold change in rhIL-2 activity is necessary in order to functionally modulate fate decisions in T cells that lead to either the memory or effector fate,[31] thus the near three logs of dynamic range observed here in vitro suggest that latent cytokines may be used to control T cell biology ex vivo or modulate therapeutic activity of the recombinant protein. To further demonstrate the feasibility of this approach, we also examined latency induction with rhIL-15, finding that small molecule linker addition, alone, was sufficient to achieve 5- to 20-fold modulation of CTLL-2 T cell dose-dependent proliferation (24 h, Figure S4).

To further explore the therapeutic potential of latent IL-2, we investigated its ability to promote antigen-specific immunity using OT-I T cell receptor transgenic mice, which generate clonal CD8$^+$ T cells specific to SIINFEKL, an octameric peptide from ovalbumin ($OVA_{257-264}$).[32] We pulsed OT-I splenocytes with $OVA_{257-264}$ and treated with either wild-type or latent IL-2, with or without LED irradiation, and measured IFNγ as an indication of the extent of T cell activation. Although latent IL-2 had no significant effect on antigen-specific T cell activation, that from the light-uncaged protein was comparable and statistically indistinguishable from wild-type IL-2 (Figure 3c).

To ascertain whether the activity of latent IL-2 on OT-I T cells was, like the wild-type protein, JAK/STAT pathway dependent, we examined its effect on HEK293 cells engineered to express all three subunits of human IL-2R, JAK3, and STAT5. In response to STAT5 activation, these cells secrete alkaline phosphatase, which can be spectrophotometrically detected using a chromogenic substrate. The trends in the reporter cell response observed in these studies closely match those observed in activated OT-I T cells. Latent IL-2 induced near-baseline levels of STAT5 transcriptional activity, while that from the light-uncaged protein was comparable to that from wild-type IL-2 (Figure 3d). Together, these data support that LED irradiation can derepress IL-2 latency, promote antigen-specific immunity, and reactivate JAK/STAT pathway signaling.

Feasibility of In Situ Cytokine Derepression. Having shown that cytokine latency can be used to temporally control immune cell signaling, we sought to characterize the spatial resolution with which cytokine activity could be constrained. We prepared a latent analog of IL-2 using bovine serum albumin modified with a photolabile PEG containing a biotin tag at its distal end (Figure 4a). Following immobilization onto glass slides, irradiation through a custom photolithographic mask, and streptavidin-FITC staining, we observed spatially constrained

https://dx.doi.org/10.1021/acs.biomac.0c00264
Biomacromolecules 2020, 21, 2635−2644

protein uncaging with a resolution at or below the typical dimensions of single human immune cells (<17 μm, Figure 4b,c). These results suggest that cytokine activity can be derepressed with high spatial and temporal control using this synthetic modification approach.

To explore the effects of tissue light attenuation on latent IL-2 activation, we fabricated a series of silicone-based phantoms that mimic light transmission through human dermis, epidermis, and hypodermis at wavelengths specific to the polymer photocages described here (Figure 5a). Using these models, we examined the stability of 5 kDa PEG photocages under prolonged, aqueous storage conditions and under conditions simulating ambient indoor light exposure of superficial veins (1 mm hypodermis depth[33]). We observed high stability of aqueous solutions in cold storage with <10% total uncaging of polymer linkages after 90 days (Figure 5b). Given that many clinical products have postreconstitution shelf lives of just hours to days, the storage durations observed here appear sufficient for large-scale in vivo testing. We also observed comparably low levels of polymer cleavage under conditions mimicking nondeliberate light exposure of superficial veins over 6 weeks (<4%). These latter data suggest that polymer-induced latency may be maintained in vivo over timescales necessary for light-constrained cytokine derepression.

To model the feasibility of light-induced cytokine uncaging in vivo, we examined the activity of latent IL-2 following photoexposure through tissue phantoms modeling human skin and subcutaneous tissue. We observed near full recovery of IL-2 activity at depths corresponding to 1 mm beneath the dermis as measured by CTLL-2 T cell proliferation (Figure 5c). These findings are significant as such depths, in many cases, correspond to the minimal light attenuation experienced at human superficial veins and within transcutaneous or some trans-epithelial tumors.[33] Moreover, as the light irradiance required for activation through tissue phantoms induced only a small temperature increase (ΔT_{max} 10.0 °C, Figure 5d), heat pain responses in vivo are expected to be mild or imperceptible.[34]

DISCUSSION

Inspired by the ability of latency-binding to impart specificity to otherwise pleiotropic immune signaling proteins, here, we describe a strategy whereby chemical modification with light-sensitive polymers can be used to control the activity of cytokines in response to simple LED light exposure. In this study, we found that modification of IL-2 and IL-15 with photolabile small molecules or polymers could modulate their activity on T cells as much as two to three orders of magnitude. This ability to control the magnitude, and correspondingly the duration, of IL-2 signals is significant as (i) both strong and sustained IL-2 signaling is necessary for the induction of the $CD8^+$ effector—rather than memory—T cell fate, and (ii) as little as a tenfold change in local cytokine concentration can bias this tradeoff.[31,35] While in vivo conditions, such as limited diffusion in tissue, extracellular matrix adhesion, and lymphatic fluid transport, may necessitate a wider range of light-induced activity modulation,[36] strategies such as those described here may, in a future work, enable the optical reprogramming of fate decisions in T cells that lead to the short-term effector function at the expense of long-term memory function.

In this work, we also show that polymer-induced latency blunts corresponding JAK/STAT pathway signaling and $CD8^+$ T cell activation ex vivo and that just brief LED light exposure can be used to derepress these effects. We envision that such high spatial and temporal control of cytokine signaling can be used modulate T cell priming/expansion directly at sites of disease or at associated secondary lymphoid organs. Such strategies may also extend to chemokines, which can serve to further orchestrate effective adaptive immune responses against pathogens or tumors. Here, we achieved a minimum spatial resolution of photoactivation approaching that of a single immune cell—without the use of focusing optics—and although light scattering and diffusion would limit such dimensions in vivo, we anticipate strong feasibility to constrain cytokine activation to millimeter-scale diseased tissues and lymph nodes in future work. This supposition is also supported by tissue phantom studies performed here, showing efficient light-induced derepression at subdermal depths of as high as 1 mm, sufficient in many instances for activation within human superficial veins and within transcutaneous or some trans-epithelial disease sites.[33] Others have also demonstrated that structurally related photocages appended to solid implants can be transcutaneously photoactivated in mice,[37,38] thus we are optimistic regarding future in vivo feasibility; further testing, however, will be required to confirm recovery of activity in the present case and to also assess potential negative effects from prolonged near-UV light exposure, such as DNA damage, tissue fibrosis, or protein denaturation.

Serendipitously, we also found that polymer-induced latency, alone, biased the affinity of latent IL-2 toward IL-2Rβ (CD122) and away from IL-2Rα (CD25). As $CD8^+$ T cells express IL-2R$\beta\gamma$ and immunosuppressive Tregs constitutively express IL-2R$\alpha\beta\gamma$, these findings suggest that the latent cytokine may improve $CD8^+$/Treg ratios, which are prognostically favorable in many cancers[39] and correlate with clinical responses to an immune checkpoint blockade therapy in patients.[40] While other mechanisms of cytokine receptor subunit-biasing based on mutagenesis,[41,42] antibody complexation,[43] and de novo protein design[44] have been reported, here, we hypothesize that atypically high density of solvent-accessible lysine resides at the IL-2/IL-2Rα interface preferentially induces steric hindrance with the receptor subunit via appended polymer chains.[24]

In addition to demonstrating rapid and efficient cytokine photoactivation, we also found that polymer photocages used here were highly stable under conditions simulating both aqueous storage and venous ambient light exposure. Compared with other promising and more rapidly hydrolyzable PEG/IL-2 conjugates (e.g., NKTR-214[45]), these findings are encouraging and could lead to future integration with wearable or implanted light-delivery devices,[46−50] which modulate drug activation. Consistent with other PEGylated cytokines,[45] we found that bioinspired, polymer-induced latency was able to prolong scIL-12 plasma circulation by approximately 11-fold, potentially precluding the need for frequent, high dosing and improving tissue drug exposure in treatment settings. Although the use of synthetic polymers such as PEG here provides many advantages including low cost and a track-record of use in more than 20 systemically administered clinical therapies or countless household products, it also presents some important limitations. The detection of anti-PEG antibodies among health individuals has increased markedly in recent years, from ∼27% in 2003 to ∼42% in 2015,[51] and while pre-existing or drug-induced anti-PEG antibodies have been shown to correlate with infusion reactions and drug activity loss after multiple injections,[52] such associations are often highly drug specific. Here, we employ recombinant human proteins, which are intrinsically weakly

https://dx.doi.org/10.1021/acs.biomac.0c00264
Biomacromolecules 2020, 21, 2635−2644

immunogenic and a high degree of PEG modification in order to minimize such risks;[51] however, future studies exploring alternative latency-inducing polymers or peptides may further improve drug activity modulation or production scalability.

Although these studies are the first, to our knowledge, to demonstrate reversible, optical control of cytokines, they build upon many prior advances.[9−13,53−57] Deiters and co-workers previously demonstrated reversible photocaging strategies for enzymes based on nitrobenzyl linkages,[58] while Esser-Kahn and co-workers and Lynn et al. have demonstrated related approaches to photoactivate smaller lipopeptide Toll-like receptor (TLR) agonists.[59,60] Likewise, Garcia et al.,[61] Hubbell et al.,[62] and Wittrupp et al.[63] have recently developed affinity-targeted cytokine fusions with a high cell- or tissue-specific activity. Combining elements of these approaches, here, we describe a bioinspired strategy for polymer-induced cytokine latency and photoinduced reactivation. The work presented here provides a proof of concept that cytokine activity can be precisely regulated using light, findings that may be further improved upon through the use of additional photolabile linkers, which absorb light at wavelengths with higher tissue penetrance.[9,64−66]

In summary, we describe a generalizable strategy for light-induced cytokine derepression that can be used to spatially and temporally control the activity of otherwise pleiotropic immune signaling molecules. As research tools, the technologies described here hold great potential to improve our ability to understand, manipulate basic immune biology, and optically reprogram immune responses ex vivo and in vitro. As therapies, they could also serve as long-acting prodrugs or tissue-selective immune modulators both alone or in combination with other immunotherapies.

■ ASSOCIATED CONTENT

Supporting Information

The Supporting Information is available free of charge at https://pubs.acs.org/doi/10.1021/acs.biomac.0c00264.

Characterization of linker cleavage, conjugation schematic, spectral properties of light sources and linker compounds, and latent IL-15 activity photomodulation (PDF)

■ AUTHOR INFORMATION

Corresponding Author

Erik C. Dreaden − *Coulter Department of Biomedical Engineering, Georgia Institute of Technology and Emory University, Atlanta, Georgia 30332-0002, United States; Department of Pediatrics, Emory School of Medicine, Atlanta, Georgia 30322, United States; Aflac Cancer and Blood Disorders Center of Children's Healthcare of Atlanta, Atlanta, Georgia 30322, United States; Petit Institute for Bioengineering and Bioscience, Georgia Institute of Technology, Atlanta, Georgia 30332-0002, United States; Winship Cancer Institute of Emory University, Atlanta, Georgia 30322, United States;* orcid.org/0000-0002-4954-8443; Email: e.dreaden@emory.edu, e.dreaden@gatech.edu

Authors

Lacey A. Perdue − *Coulter Department of Biomedical Engineering, Georgia Institute of Technology and Emory University, Atlanta, Georgia 30332-0002, United States*

Priscilla Do − *Coulter Department of Biomedical Engineering, Georgia Institute of Technology and Emory University, Atlanta, Georgia 30332-0002, United States*

Camille David − *Department of Pediatrics, Emory School of Medicine, Atlanta, Georgia 30322, United States; Aflac Cancer and Blood Disorders Center of Children's Healthcare of Atlanta, Atlanta, Georgia 30322, United States; Winship Cancer Institute of Emory University, Atlanta, Georgia 30322, United States*

Andrew Chyong − *Coulter Department of Biomedical Engineering, Georgia Institute of Technology and Emory University, Atlanta, Georgia 30332-0002, United States*

Anna V. Kellner − *Coulter Department of Biomedical Engineering, Georgia Institute of Technology and Emory University, Atlanta, Georgia 30332-0002, United States*

Amanda Ruggieri − *Department of Hematology and Medical Oncology, Emory School of Medicine, Atlanta, Georgia 30322, United States; Winship Cancer Institute of Emory University, Atlanta, Georgia 30322, United States*

Hye Ryong Kim − *Coulter Department of Biomedical Engineering, Georgia Institute of Technology and Emory University, Atlanta, Georgia 30332-0002, United States*

Khalid Salaita − *Department of Chemistry, Emory University, Atlanta, Georgia 30322, United States; Coulter Department of Biomedical Engineering, Georgia Institute of Technology and Emory University, Atlanta, Georgia 30332-0002, United States;* orcid.org/0000-0003-4138-3477

Gregory B. Lesinski − *Department of Hematology and Medical Oncology, Emory School of Medicine, Atlanta, Georgia 30322, United States; Winship Cancer Institute of Emory University, Atlanta, Georgia 30322, United States*

Christopher C. Porter − *Department of Pediatrics, Emory School of Medicine, Atlanta, Georgia 30322, United States; Aflac Cancer and Blood Disorders Center of Children's Healthcare of Atlanta, Atlanta, Georgia 30322, United States; Winship Cancer Institute of Emory University, Atlanta, Georgia 30322, United States*

Complete contact information is available at: https://pubs.acs.org/10.1021/acs.biomac.0c00264

Author Contributions

L.A.P., P.D., K.S., G.B.L., C.C.P., and E.C.D. designed research; L.A.P., P.D., C.D., A.C., A.V.K., A.R., H.K., K.S., G.B.L., C.C.P, and E.C.D. performed research or analyzed data; and L.A.P., C.C.P., and E.C.D. wrote the manuscript.

Notes

The authors declare no competing financial interest.

■ ACKNOWLEDGMENTS

This work was supported in part by the American Cancer Society (#IRG-17-181-04), the Winship Cancer Institute, the National Institutes of Health Research Training Program in Immunoengineering (T32EB021962; F31CA243502), the AAI Careers in Immunology Fellowship Program, the Coulter Department of Biomedical Engineering, and the Aflac Cancer and Blood Disorders Center of Children's Healthcare of Atlanta. We are also grateful for assistance from the Children's Healthcare of Atlanta and Emory University's Pediatric Integrated Cellular Imaging Core and Pediatric General Equipment and Specimen Processing Core, the Robert P. Apkarian Integrated Electron Microscopy Core, and the Emory Chemical Biology Discovery Center. The content here is solely the responsibility of the authors and does not necessarily represent the official views of the Winship Cancer Institute, Aflac

Inc., Children's Healthcare of Atlanta, or the National Institutes of Health.

REFERENCES

(1) Grivennikov, S. I.; Greten, F. R.; Karin, M. Immunity, Inflammation, and Cancer. *Cell* **2010**, *140*, 883−899.

(2) Dranoff, G. Cytokines in cancer pathogenesis and cancer therapy. *Nat. Rev. Cancer* **2004**, *4*, 11−22.

(3) Watowich, S. S.; Wu, H.; Socolovsky, M.; Klingmuller, U.; Constantinescu, S. N.; Lodish, H. F. Cytokine Receptor Signal Transduction and the Control of Hematopoietic Cell Development. *Annu. Rev. Cell Dev. Biol.* **1996**, *12*, 91−128.

(4) Moraga, I.; Spangler, J.; Mendoza, J. L.; Garcia, K. C. Chapter One - Multifarious Determinants of Cytokine Receptor Signaling Specificity. In *Adv. Immunol.*; Alt, F. W., Ed. Academic Press, 2014; Vol. *121*, pp 1−39.

(5) Dong, X.; Zhao, B.; Iacob, R. E.; Zhu, J.; Koksal, A. C.; Lu, C.; Engen, J. R.; Springer, T. A. Force interacts with macromolecular structure in activation of TGF-β. *Nature* **2017**, *542*, 55.

(6) Mani, V.; Bromley, S. K.; Äijö, T.; Mora-Buch, R.; Carrizosa, E.; Warner, R. D.; Hamze, M.; Sen, D. R.; Chasse, A. Y.; Lorant, A.; Griffith, J. W.; Rahimi, R. A.; McEntee, C. P.; Jeffrey, K. L.; Marangoni, F.; Travis, M. A.; Lacy-Hulbert, A.; Luster, A. D.; Mempel, T. R. Migratory DCs activate TGF-β to precondition naïve CD8+ T cells for tissue-resident memory fate. *Science* **2019**, *366*, No. eaav5728.

(7) Liénart, S.; Merceron, R.; Vanderaa, C.; Lambert, F.; Colau, D.; Stockis, J.; van der Woning, B.; De Haard, H.; Saunders, M.; Coulie, P. G.; Savvides, S. N.; Lucas, S. Structural basis of latent TGF-β1 presentation and activation by GARP on human regulatory T cells. *Science* **2018**, *362*, 952−956.

(8) Qin, Y.; Garrison, B. S.; Ma, W.; Wang, R.; Jiang, A.; Li, J.; Mistry, M.; Bronson, R. T.; Santoro, D.; Franco, C.; Robinton, D. A.; Stevens, B.; Rossi, D. J.; Lu, C.; Springer, T. A. A Milieu Molecule for TGF-β Required for Microglia Function in the Nervous System. *Cell* **2018**, *174*, 156−171.e16.

(9) Szymański, W.; Beierle, J. M.; Kistemaker, H. A. V.; Velema, W. A.; Feringa, B. L. Reversible Photocontrol of Biological Systems by the Incorporation of Molecular Photoswitches. *Chem. Rev* **2013**, *113*, 6114−6178.

(10) Ankenbruck, N.; Courtney, T.; Naro, Y.; Deiters, A. Optochemical Control of Biological Processes in Cells and Animals. *Angew. Chem., Int. Ed.* **2018**, *57*, 2768−2798.

(11) Matsuzaki, M.; Honkura, N.; Ellis-Davies, G. C. R.; Kasai, H. Structural basis of long-term potentiation in single dendritic spines. *Nature* **2004**, *429*, 761−766.

(12) Chauveau, A.; Le Floc'h, A.; Bantilan, N. S.; Koretzky, G. A.; Huse, M. Diacylglycerol kinase α establishes T cell polarity by shaping diacylglycerol accumulation at the immunological synapse. *Sci. Signal.* **2014**, *7*, ra82−ra82.

(13) Jain, P. K.; Ramanan, V.; Schepers, A. G.; Dalvie, N. S.; Panda, A.; Fleming, H. E.; Bhatia, S. N. Development of Light-Activated CRISPR Using Guide RNAs with Photocleavable Protectors. *Angew. Chem., Int. Ed.* **2016**, *55*, 12440−12444.

(14) Ayers, F.; Grant, A.; Kuo, D.; Cuccia, D.; Durkin, A. J. Fabrication and characterization of silicone-based tissue phantoms with tunable optical properties in the visible and near infrared domain. *SPIE BiOS* **2008**, *6870*, 6870071−6870079.

(15) Saager, R.; Kondru, C.; Au, K.; Sry, K.; Ayers, F.; Durkin, A. J. Multilayer silicone phantoms for the evaluation of quantitative optical techniques in skin imaging. *SPIE BiOS* **2010**, *7567*, 7567061−7567068.

(16) Choe, R. Diffuse optical tomography and spectroscopy of breast cancer and fetal brain. *Med. Phys.* **2005**, *32*, 3230−3230.

(17) Bashkatov, A. N.; Genina, E. A.; Tuchin, V. V. Optical Properties of Skin, Subcutaneous, and Muscle Tissues: A Review. *J. Innov. Opt. Health Sci.* **2011**, *04*, 9−38.

(18) Polukhtin, A.; Walsh, P. L. Compounds and Methods for Detection and Isolation of Biomolecules. US Patent App. 14,789,784, 2016.

(19) Patchornik, A.; Amit, B.; Woodward, R. B. Photosensitive protecting groups. *J. Am. Chem. Soc.* **1970**, *92*, 6333−6335.

(20) Bochet, C. G. Photolabile protecting groups and linkers. *J. Chem. Soc., Perkin Trans. 1* **2002**, *2*, 125−142.

(21) Boyman, O.; Sprent, J. The role of interleukin-2 during homeostasis and activation of the immune system. *Nat. Rev. Immunol.* **2012**, *12*, 180−190.

(22) Abbas, A. K.; Trotta, E.; Simeonov, D. R.; Marson, A.; Bluestone, J. A. Revisiting IL-2: Biology and therapeutic prospects. *Sci. Immunol.* **2018**, *3*, No. eaat1482.

(23) Fitzgerald, K. A.; O'Neill, L. A. J.; Gearing, A. J. H.; Callard, R. E. IL-2. In *The Cytokine FactsBook and Webfacts*; (2 nd Edition) Fitzgerald, K. A.; O'Neill, L. A. J.; Gearing, A. J. H.; Callard, R. E., Eds. *Academic Press: London*, 2001; pp 44−50.

(24) Charych, D. H.; Hoch, U.; Langowski, J. L.; Lee, S. R.; Addepalli, M. K.; Kirk, P. B.; Sheng, D.; Liu, X.; Sims, P. W.; VanderVeen, L. A.; Ali, C. F.; Chang, T. K.; Konakova, M.; Pena, R. L.; Kanhere, R. S.; Kirksey, Y. M.; Ji, C.; Wang, Y.; Huang, J.; Sweeney, T. D.; Kantak, S. S.; Doberstein, S. K. NKTR-214, an Engineered Cytokine with Biased IL2 Receptor Binding, Increased Tumor Exposure, and Marked Efficacy in Mouse Tumor Models. *Clin. Cancer Res.* **2016**, *22*, 680−690.

(25) Sim, G. C.; Martin-Orozco, N.; Jin, L.; Yang, Y.; Wu, S.; Washington, E.; Sanders, D.; Lacey, C.; Wang, Y.; Vence, L.; Hwu, P.; Radvanyi, L. IL-2 therapy promotes suppressive ICOS+ Treg expansion in melanoma patients. *J. Clin. Invest.* **2014**, *124*, 99−110.

(26) Lasek, W.; Zagożdżon, R.; Jakobisiak, M. Interleukin 12: still a promising candidate for tumor immunotherapy? *Cancer Immunol. Immunother.* **2014**, *63*, 419−435.

(27) Alconcel, S. N. S.; Baas, A. S.; Maynard, H. D. FDA-approved poly(ethylene glycol)−protein conjugate drugs. *Polym. Chem.* **2011**, *2*, 1442−1448.

(28) Xie, T.; Fang, H.; Ouyang, W.; Angart, P.; Chiang, M.-J.; Bhirde, A. A.; Sheikh, F.; Lynch, P.; Shah, A. B.; Patil, S. M.; Chen, K.; Shen, M.; Agarabi, C.; Donnelly, R. P.; Brorson, K.; Schrieber, S. J.; Howard, K. E.; Rogstad, S. M.; Frucht, D. M. The ELISA Detectability and Potency of Pegfilgrastim Decrease in Physiological Conditions: Key Roles for Aggregation and Individual Variability. *Sci. Rep.* **2020**, *10*, 2476.

(29) Carmenate, T.; Pacios, A.; Enamorado, M.; Moreno, E.; Garcia-Martínez, K.; Fuente, D.; León, K. Human IL-2 Mutein with Higher Antitumor Efficacy Than Wild Type IL-2. *J. Immunol.* **2013**, *190*, 6230−6238.

(30) Fan, P. L.; Schumacher, R. M.; Azzolin, K.; Geary, R.; Eichmiller, F. C. Curing-light intensity and depth of cure of resin-based composites tested according to international standards. *J. Am. Dent. Assoc.* **2002**, *133*, 429−434.

(31) Pipkin, M. E.; Sacks, J. A.; Cruz-Guilloty, F.; Lichtenheld, M. G.; Bevan, M. J.; Rao, A. Interleukin-2 and Inflammation Induce Distinct Transcriptional Programs that Promote the Differentiation of Effector Cytolytic T Cells. *Immunity* **2010**, *32*, 79−90.

(32) Werlen, G.; Hausmann, B.; Palmer, E. A motif in the $\alpha\beta$ T-cell receptor controls positive selection by modulating ERK activity. *Nature* **2000**, *406*, 422−426.

(33) Goh, C. M.; Subramaniam, R.; Saad, N. M.; Ali, S. A.; Meriaudeau, F. Subcutaneous veins depth measurement using diffuse reflectance images. *Opt. Express* **2017**, *25*, 25741−25759.

(34) Yarnitsky, D.; Sprecher, E.; Zaslansky, R.; Hemli, J. A. Heat pain thresholds: normative data and repeatability. *Pain* **1995**, *60*, 329−332.

(35) Kalia, V.; Sarkar, S.; Subramaniam, S.; Haining, W. N.; Smith, K. A.; Ahmed, R. Prolonged Interleukin-2Rα Expression on Virus-Specific CD8+ T Cells Favors Terminal-Effector Differentiation In Vivo. *Immunity* **2010**, *32*, 91−103.

(36) Yang, R.; Wei, T.; Goldberg, H.; Wang, W.; Cullion, K.; Kohane, D. S. Getting Drugs Across Biological Barriers. *Adv. Mater.* **2017**, *29*, 1606596.

(37) Lee, T. T.; García, J. R.; Paez, J. I.; Singh, A.; Phelps, E. A.; Weis, S.; Shafiq, Z.; Shekaran, A.; del Campo, A.; García, A. J. Light-triggered in vivo activation of adhesive peptides regulates cell adhesion, inflammation and vascularization of biomaterials. *Nature Mater.* **2015**, *14*, 352−360.

https://dx.doi.org/10.1021/acs.biomac.0c00264
Biomacromolecules 2020, 21, 2635−2644

(38) Sarode, B. R.; Kover, K.; Tong, P. Y.; Zhang, C.; Friedman, S. H. Light Control of Insulin Release and Blood Glucose Using an Injectable Photoactivated Depot. *Mol. Pharmaceutics* **2016**, *13*, 3835−3841.
(39) Sato, E.; Olson, S. H.; Ahn, J.; Bundy, B.; Nishikawa, H.; Qian, F.; Jungbluth, A. A.; Frosina, D.; Gnjatic, S.; Ambrosone, C.; Kepner, J.; Odunsi, T.; Ritter, G.; Lele, S.; Chen, Y.-T.; Ohtani, H.; Old, L. J.; Odunsi, K. Intraepithelial CD8+ tumor-infiltrating lymphocytes and a high CD8+/regulatory T cell ratio are associated with favorable prognosis in ovarian cancer. *Proc. Natl. Acad. Sci. U. S. A.* **2005**, *102*, 18538−18543.
(40) Hodi, F. S.; Butler, M.; Oble, D. A.; Seiden, M. V.; Haluska, F. G.; Kruse, A.; MacRae, S.; Nelson, M.; Canning, C.; Lowy, I.; Korman, A.; Lautz, D.; Russell, S.; Jaklitsch, M. T.; Ramaiya, N.; Chen, T. C.; Neuberg, D.; Allison, J. P.; Mihm, M. C.; Dranoff, G. Immunologic and clinical effects of antibody blockade of cytotoxic T lymphocyte-associated antigen 4 in previously vaccinated cancer patients. *Proc. Natl. Acad. Sci. U. S. A.* **2008**, *105*, 3005−3010.
(41) Levin, A. M.; Bates, D. L.; Ring, A. M.; Krieg, C.; Lin, J. T.; Su, L.; Moraga, I.; Raeber, M. E.; Bowman, G. R.; Novick, P.; Pande, V. S.; Fathman, C. G.; Boyman, O.; Garcia, K. C. Exploiting a natural conformational switch to engineer an interleukin-2 'superkine'. *Nature* **2012**, *484*, 529−533.
(42) Gillies, S. D.; Lan, Y.; Hettmann, T.; Brunkhorst, B.; Sun, Y.; Mueller, S. O.; Lo, K.-M. A Low-Toxicity IL-2−Based Immunocytokine Retains Antitumor Activity Despite Its High Degree of IL-2 Receptor Selectivity. *Clin. Cancer Res.* **2011**, *17*, 3673−3685.
(43) Krieg, C.; Létourneau, S.; Pantaleo, G.; Boyman, O. Improved IL-2 immunotherapy by selective stimulation of IL-2 receptors on lymphocytes and endothelial cells. *Proc. Natl. Acad. Sci. U. S. A.* **2010**, *107*, 11906−11911.
(44) Silva, D.-A.; Yu, S.; Ulge, U. Y.; Spangler, J. B.; Jude, K. M.; Labão-Almeida, C.; Ali, L. R.; Quijano-Rubio, A.; Ruterbusch, M.; Leung, I.; Biary, T.; Crowley, S. J.; Marcos, E.; Walkey, C. D.; Weitzner, B. D.; Pardo-Avila, F.; Castellanos, J.; Carter, L.; Stewart, L.; Riddell, S. R.; Pepper, M.; Bernardes, G. J. L.; Dougan, M.; Garcia, K. C.; Baker, D. De novo design of potent and selective mimics of IL-2 and IL-15. *Nature* **2019**, *565*, 186−191.
(45) Charych, D.; Khalili, S.; Dixit, V.; Kirk, P.; Chang, T.; Langowski, J.; Rubas, W.; Doberstein, S. K.; Eldon, M.; Hoch, U.; Zalevsky, J. Modeling the receptor pharmacology, pharmacokinetics, and pharmacodynamics of NKTR-214, a kinetically-controlled interleukin-2 (IL2) receptor agonist for cancer immunotherapy. *PLoS One* **2017**, *12*, No. e0179431.
(46) Bagley, A. F.; Hill, S.; Rogers, G. S.; Bhatia, S. N. Plasmonic Photothermal Heating of Intraperitoneal Tumors through the Use of an Implanted Near-Infrared Source. *ACS Nano* **2013**, *7*, 8089−8097.
(47) Nizamoglu, S.; Gather, M. C.; Humar, M.; Choi, M.; Kim, S.; Kim, K. S.; Hahn, S. K.; Scarcelli, G.; Randolph, M.; Redmond, R. W.; Yun, S. H. Bioabsorbable polymer optical waveguides for deep-tissue photomedicine. *Nat. Commun.* **2016**, *7*, 10374.
(48) Mickle, A. D.; Won, S. M.; Noh, K. N.; Yoon, J.; Meacham, K. W.; Xue, Y.; McIlvried, L. A.; Copits, B. A.; Samineni, V. K.; Crawford, K. E.; Kim, D. H.; Srivastava, P.; Kim, B. H.; Min, S.; Shiuan, Y.; Yun, Y.; Payne, M. A.; Zhang, J.; Jang, H.; Li, Y.; Lai, H. H.; Huang, Y.; Park, S.-I.; Gereau, R. W., IV; Rogers, J. A. A wireless closed-loop system for optogenetic peripheral neuromodulation. *Nature* **2019**, *565*, 361−365.
(49) Kim, J.; Salvatore, G. A.; Araki, H.; Chiarelli, A. M.; Xie, Z.; Banks, A.; Sheng, X.; Liu, Y.; Lee, J. W.; Jang, K.-I.; Heo, S. Y.; Cho, K.; Luo, H.; Zimmerman, B.; Kim, J.; Yan, L.; Feng, X.; Xu, S.; Fabiani, M.; Gratton, G.; Huang, Y.; Paik, U.; Rogers, J. A. Battery-free, stretchable optoelectronic systems for wireless optical characterization of the skin. *Sci. Adv.* **2016**, *2*, No. e1600418.
(50) Choi, M.; Choi, J. W.; Kim, S.; Nizamoglu, S.; Hahn, S. K.; Yun, S. H. Light-guiding hydrogels for cell-based sensing and optogenetic synthesis in vivo. *Nat. Photonics* **2013**, *7*, 987−994.
(51) Zhang, P.; Sun, F.; Liu, S.; Jiang, S. Anti-PEG antibodies in the clinic: Current issues and beyond PEGylation. *J. Controlled Release* **2016**, *244*, 184−193.
(52) Ishida, T.; Ichihara, M.; Wang, X.; Yamamoto, K.; Kimura, J.; Majima, E.; Kiwada, H. Injection of PEGylated liposomes in rats elicits PEG-specific IgM, which is responsible for rapid elimination of a second dose of PEGylated liposomes. *J. Controlled Release* **2006**, *112*, 15−25.
(53) Nani, R. R.; Gorka, A. P.; Nagaya, T.; Yamamoto, T.; Ivanic, J.; Kobayashi, H.; Schnermann, M. J. In Vivo Activation of Duocarmycin−Antibody Conjugates by Near-Infrared Light. *ACS Cent. Sci.* **2017**, *3*, 329−337.
(54) Döbber, A.; Phoa, A. F.; Abbassi, R. H.; Stringer, B. W.; Day, B. W.; Johns, T. G.; Abadleh, M.; Peifer, C.; Munoz, L. Development and Biological Evaluation of a Photoactivatable Small Molecule Microtubule-Targeting Agent. *ACS Med. Chem. Lett.* **2017**, *8*, 395−400.
(55) Kobayashi, H.; Choyke, P. L. Near-Infrared Photoimmunotherapy of Cancer. *Acc. Chem. Res.* **2019**, *52*, 2332−2339.
(56) Lin, E.-W.; Boehnke, N.; Maynard, H. D. Protein−Polymer Conjugation via Ligand Affinity and Photoactivation of Glutathione S-Transferase. *Bioconjugate Chem.* **2014**, *25*, 1902−1909.
(57) Tang, L.; Zheng, Y.; Melo, M. B.; Mabardi, L.; Castaño, A. P.; Xie, Y.-Q.; Li, N.; Kudchodkar, S. B.; Wong, H. C.; Jeng, E. K.; Maus, M. V.; Irvine, D. J. Enhancing T cell therapy through TCR-signaling-responsive nanoparticle drug delivery. *Nat. Biotechnol.* **2018**, *36*, 707−716.
(58) Georgianna, W. E.; Lusic, H.; McIver, A. L.; Deiters, A. Photocleavable Polyethylene Glycol for the Light-Regulation of Protein Function. *Bioconjugate Chem.* **2010**, *21*, 1404−1407.
(59) Mancini, R. J.; Stutts, L.; Moore, T.; Esser-Kahn, A. P. Controlling the Origins of Inflammation with a Photoactive Lipopeptide Immunopotentiator. *Angew. Chem., Int. Ed.* **2015**, *54*, 5962−5965.
(60) Lynn, G. M.; Laga, R.; Darrah, P. A.; Ishizuka, A. S.; Balaci, A. J.; Dulcey, A. E.; Pechar, M.; Pola, R.; Gerner, M. Y.; Yamamoto, A.; Buechler, C. R.; Quinn, K. M.; Smelkinson, M. G.; Vanek, O.; Cawood, R.; Hills, T.; Vasalatiy, O.; Kastenmüller, K.; Francica, J. R.; Stutts, L.; Tom, J. K.; Ryu, K. A.; Esser-Kahn, A. P.; Etrych, T.; Fisher, K. D.; Seymour, L. W.; Seder, R. A. In vivo characterization of the physicochemical properties of polymer-linked TLR agonists that enhance vaccine immunogenicity. *Nat. Biotechnol.* **2015**, *33*, 1201−1210.
(61) Spangler, J. B.; Trotta, E.; Tomala, J.; Peck, A.; Young, T. A.; Savvides, C. S.; Silveria, S.; Votavova, P.; Salafsky, J.; Pande, V. S.; Kovar, M.; Bluestone, J. A.; Garcia, K. C. Engineering a Single-Agent Cytokine/Antibody Fusion That Selectively Expands Regulatory T Cells for Autoimmune Disease Therapy. *J. Immunol.* **2018**, *201*, 2094−2106.
(62) Ishihara, J.; Ishihara, A.; Sasaki, K.; Lee, S. S.-Y.; Williford, J.-M.; Yasui, M.; Abe, H.; Potin, L.; Hosseinchi, P.; Fukunaga, K.; Raczy, M. M.; Gray, L. T.; Mansurov, A.; Katsumata, K.; Fukayama, M.; Kron, S. J.; Swartz, M. A.; Hubbell, J. A. Targeted antibody and cytokine cancer immunotherapies through collagen affinity. *Sci. Transl. Med.* **2019**, *11*, No. eaau3259.
(63) Momin, N.; Mehta, N. K.; Bennett, N. R.; Ma, L.; Palmeri, J. R.; Chinn, M. M.; Lutz, E. A.; Kang, B.; Irvine, D. J.; Spranger, S.; Wittrup, K. D. Anchoring of intratumorally administered cytokines to collagen safely potentiates systemic cancer immunotherapy. *Sci. Transl. Med.* **2019**, *11*, No. eaaw2614.
(64) Peterson, J. A.; Wijesooriya, C.; Gehrmann, E. J.; Mahoney, K. M.; Goswami, P. P.; Albright, T. R.; Syed, A.; Dutton, A. S.; Smith, E. A.; Winter, A. H. Family of BODIPY Photocages Cleaved by Single Photons of Visible/Near-Infrared Light. *J. Am. Chem. Soc.* **2018**, *140*, 7343−7346.
(65) Riley, R. S.; Dang, M. N.; Billingsley, M. M.; Abraham, B.; Gundlach, L.; Day, E. S. Evaluating the Mechanisms of Light-Triggered siRNA Release from Nanoshells for Temporal Control Over Gene Regulation. *Nano Lett.* **2018**, *18*, 3565−3570.
(66) Wang, J.; Potocny, A. M.; Rosenthal, J.; Day, E. S. Gold Nanoshell-Linear Tetrapyrrole Conjugates for Near Infrared-Activated Dual Photodynamic and Photothermal Therapies. *ACS Omega* **2020**, *5*, 926−940.

https://dx.doi.org/10.1021/acs.biomac.0c00264
Biomacromolecules 2020, 21, 2635−2644